

Scratch and recovery characteristics of automotive clearcoats containing blocked polyisocyanate crosslinkers

Seung Man Noh, Joon Hyun Nam, Jung Kwon Oh,
Hyun Wook Jung

© American Coatings Association 2014

Abstract Scratch characteristics and self-recovery behaviors of automotive clearcoats including newly designed silane-modified blocked polyisocyanate (SMBI)¹ as an organic–inorganic hybrid crosslinker were compared with those with the commercially well-known crosslinkers such as blocked HDI-based and blocked IPDI-based polyisocyanates. To extensively scrutinize the effects of various crosslinkers with different chemical structures on the chemical and mechanical properties of clearcoats themselves, rigid-body pendulum tester analysis, creep-recovery analysis, and FTIR analysis were performed, resulting in a noticeable variation in curing features and crosslinking networks. Employing the overall coating systems by depositing clearcoats with different crosslinkers above the same undercoats on galvanized steel, the scratch behaviors on the surface of the outermost clearcoat layer were examined via the nano-scratch tester for scratch depth profiles and atomic force microscopy for three-dimensional scratch images, under various self-reflow temperatures and duration time periods. The results demonstrated that the SMBI crosslinker induced a considerably higher degree of crosslinked networks, through the reaction of urethane bonds and

silanol bonds in clearcoats, in comparison with the blocked HDI and IPDI polyisocyanates. Also, the recoverable behaviors of scratched clearcoats containing different blocked polyisocyanates were affected by the intrinsic chemical structures of crosslinkers, as well as scratch-recovery conditions such as external temperatures and duration times.

Keywords Silane-modified blocked polyisocyanate, Self-reflow, Clearcoats, Scratch recovery

Introduction

Today's automotive clearcoats, with their splendid appearances, are expected to undergo a variety of severe environmental stresses without exhibiting permanent damage. One intensive environmental stress is the dynamic mechanical force that causes significant scratch and mar damage on a clearcoat surface, deteriorating the high-gloss appearance of clearcoats. Marring is a kind of physical damage that occurs within a few micrometers of the surface, and a scratch is a severe kind of marring that can be more obtrusive, owing to the wet-look exterior of automotive coatings. These minute scratches, in particular, are significantly detrimental to a glossy visual effect. Recently, both scratch and mar damages have been recognized as serious environmentally related coating defects, inducing not only major concerns for consumers but also warranty issues for automotive industries.^{2–14}

Thus, extensive research studies have been explored to formulate clearcoats with better scratch-resistant properties and also to develop ingenious technologies for the characterization of scratch and mar resistance. Most previous works have focused on trying to optimally design clearcoat formulations in terms of the improvement of scratch resistance by increasing crosslink density within polymer networks,^{15–19} the

S. M. Noh, H. W. Jung (✉)
Department of Chemical and Biological Engineering,
Korea University, Seoul 136-713, Republic of Korea
e-mail: hwjung@grtrkr.korea.ac.kr

S. M. Noh, J. H. Nam
Research Center for Green Fine Chemicals, Korea
Research Institute of Chemical Technology,
Ulsan 681-310, Republic of Korea

J. K. Oh (✉)
Department of Chemistry and Biochemistry,
Center for Nanoscience Research (CENR),
Concordia University, Montreal, QC H4B 1R6, Canada
e-mail: john.oh@concordia.ca

Table 1: Formulations of clearcoats with SMBI, blocked HDI-based, and blocked IPDI-based polyisocyanates

No	Contents	NV (%)	H	H-1	H-2	H-3	I	I-1	I-2	I-3	J	J-1	J-2	J-3
1	Butyl acetate		5	5	5	5	5	5	5	5	5	5	5	5
2	Xylene		4	4	4	4	4	4	4	4	4	4	4	4
3	Tinuvin 400/292		1.5	1.5	1.5	1.5	1.5	1.5	1.5	1.5	1.5	1.5	1.5	1.5
4	Setalux 1756 VV-65	65	37	37	37	37	37	37	37	37	37	37	37	37
5	Setalux 91772 SS-60	60	18	18	18	18	18	18	18	18	18	18	18	18
6	Setamine US 138BB-70	70	24	19.5	15.5	11	24	19.5	15.5	11	24	19.5	15.5	11
7	Desmodur PL-350 (HDI-based)	75					2.7	5.3	8	10.7				
8	Desmodur BL-4265 (IPDI-based)	65									4	8	12	16
9	Vestanat BS 1940/1 (SMBI-based)	80	3.8	7.5	11.2	15								
10	Baysilon OL 10% solution		0.5	0.5	0.5	0.5	0.5	0.5	0.5	0.5	0.5	0.5	0.5	0.5
11	Solvesso 100		6.2	7	7.3	8	7.3	9.2	10.5	12.3	6	6.5	6.5	7
Total			100	100	100	100	100	100	100	100	100	100	100	100
Nonvolatiles (wt%)			50.5	51.0	51.4	51.9	50.0	50.1	50.0	50.0	51.4	51.7	51.3	51.8
Equivalent of NCO			0.005	0.010	0.015	0.020	0.005	0.010	0.015	0.020	0.005	0.010	0.015	0.020
AC:Mel (based on solid)			2.07	2.55	3.21	4.53	2.07	2.55	3.21	4.53	2.07	2.55	3.21	4.53

addition of nano-particles,^{20,21} or self-healing technologies using new chemically modified materials.^{22–24} Increased crosslinking has been shown to enhance the intrinsic strength of the polymer networks of clearcoats, and thereby augment scratch resistance to plastic deformation; however, these changes would also be accompanied by increased brittleness of the clearcoat via a reduction in its toughness or yield to external stresses. The use of inorganic particles in the nano-scale range can be especially attractive since it allows for the improvement of the scratch-resistant properties of clearcoats by controlling surface modification.

In the previous study,¹ we investigated the scratch characteristics of silane-modified blocked polyisocyanate (SMBI) crosslinker on acrylic polyol resin with butylated melamine for clearcoats, containing dual-functional groups based on blocked polyisocyanate groups as the organic moiety, and alkoxy silane groups as the inorganic moiety. These clearcoats had considerable hybrid cross-linking networks due to the urethane and silanol bonds of the SMBI, which provided superior scratch resistance through the nano-scratch, Amtec-Kistler car-wash, and Crockmeter tests. The scratch patterns on the clearcoat surface mainly depended upon plastic deformation rather than fracture deformation under conditions from low to high external shear loads.^{1,25,26} It was substantiated that SMBI considerably enhanced the mechanical properties of clearcoats through the increased formation of cross-linking networks, and that such properties could be positively competitive with those by commercialized blocked polyisocyanates.

In this study, the scratch characteristics and self-recovery behaviors of clearcoats by SMBI crosslinker have been systematically compared with those by commercially well-known blocked polyisocyanate crosslinkers, in particular, blocked hexamethylene diisocyanate (HDI) and blocked isophorone diisocyanate (IPDI) polyisocyanates, under equivalent amounts of NCO and nonvolatiles. The influence of crosslinkers with different chemical structures in clearcoats themselves on curing behaviors and physical properties was also figured out by means of the rigid-body pendulum test (RPT), FTIR, and the creep-recovery test. Additionally, for the overall coating systems with outermost clearcoats above undercoats of primer and basecoat on galvanized steel, the comparison of scratch patterns on the clearcoat surface was accomplished using nano-scratch tests under various self-reflow conditions such as temperatures from room temperature to 50, 70, and 90°C, and duration time conditions of 1 or 2 h. Scratch images were simultaneously visualized on three-dimensional scratch profiles by atomic force microscopy (AFM).

Experimental

Preparation of clearcoat samples

In order to effectively maintain the comparability of clearcoat formulations with the previous case,¹ they were

prepared in the same way, using the same acrylic polyols (Setalux 1756 VV-65 with 90 mg KOH/g and Setalux 91772 SS-60 with 150 mg KOH/g from Nuplex) and butylated melamine (Setamine US 138 BB-70, Nuplex) as listed in Table 1. A total of 12 different clearcoats were formulated including SMBI (Vestanat BS-1940/1, Evonik) designated by H to H-3, HDI (Desmodur PL-350, Bayer) designated by I to I-3, and IPDI (Desmodur BL-4265, Bayer) designated by J to J-3,^{27–31} respectively. In particular, the ratios of acrylic to melamine resins in clearcoat samples containing three different blocked polyisocyanate crosslinkers were varied from 2.07 to 2.55, 3.21, and 4.53. The ratios of butylated melamine to three different blocked polyisocyanates were changed to examine the effect of each crosslinker on the physical properties of clearcoats under the fixed solid content of acrylic polyols. Tinuvin 400 (BASF SE) was added as a UV absorber (UVA), and Tinuvin 292 was used as a hindered amine light stabilizer (HALS). A small portion of Baysilon OL (Bayer AG) as a silicone oil was included for surface leveling.

The above clearcoats themselves were directly utilized for RPT, FTIR, and creep tests, as will be described in the next section. In particular, conventional automotive OEM coating systems were applied for nano-scratch tests to clearly capture the scratch damages of the outermost clearcoat layer. Galvanized steel panels were first phosphated and then electrocoated with a standard epoxy-based electrodeposition paint to a thickness of approximately 20 to 22 μm . The conventional dark-gray solventborne primer and waterborne black basecoat supported from PPG Industries were subsequently deposited on the electrocoated panels in series with thicknesses of 30 to 33 μm and 10 to 13 μm , respectively, using the pneumatic spray-coating method. Finally, the clearcoats prepared for this study were sprayed on the basecoat layer with 40 to 50 μm thickness and then cured at 140°C for 20 min. Physical characteristics of the cured clearcoats were measured, after keeping them at room temperature for 24 h.

Characterization methods

Curing analysis using RPT

To analyze the crosslinked network structure and reaction rates of clearcoats, an RPT (RPT-3000 W, A&D, Japan) was utilized on the basis of ISO 12013-1 and 12013-2. This is a useful and easy tool to monitor the change of physical properties of clearcoats during various thermal curing operations in the wide temperature range from -100 to $+400^\circ\text{C}$. A knife-edge pendulum was installed to determine variation in pendulum periods from oscillating patterns of the pendulum driven by magnetic force, directly grasping the variation in surface properties caused by the evolution of chemical and physical crosslinked networks inside clearcoats. More detailed descriptions for RPT equipment have been introduced in other studies.^{1,18,32} In this study, the

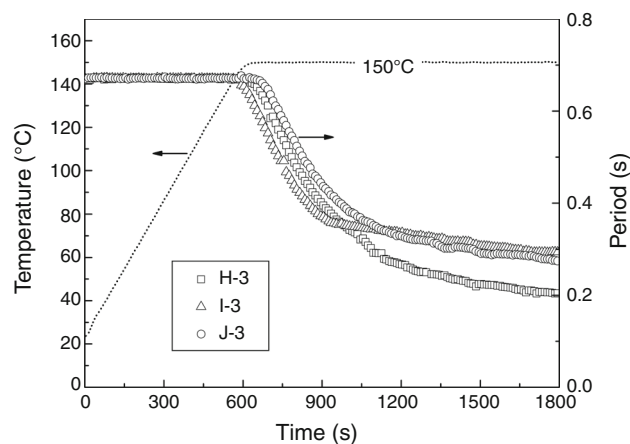


Fig. 1: The curing behavior of clearcoat samples H-3, I-3, and J-3 using a rigid-body pendulum tester at 150°C

curing temperature inside the RPT's heating chamber was gradually raised from room temperature to 140°C at a rate of 23.4°C/min and then maintained at a slightly elevated 150°C for the curing behavior measurement. For this test, the average film thickness was 40 to 50 μm .

FTIR analysis

In order to verify the evidence of chemical reactions in the prepared clearcoats between the hydroxyl functional groups on the acrylic polyol and isocyanate, and the modified silane functional groups of the SMBI, an FTIR technique was performed using a Spectrum 100 (Perkin Elmer, USA), based on attenuated total reflection (ATR) technology. In this way, chemical reactions by three different polyisocyanate molecules were illuminated via FTIR analysis as follows. The absorption bands at 2270 cm^{-1} for $-\text{NCO}$, 1720 cm^{-1} for $-\text{NHCO}$, 1690 cm^{-1} for $-\text{NHCOO}$, and 1080 cm^{-1} for $-\text{Si-O-Si-}$ assure the reaction between the acrylic polyol and three different polyisocyanates. Note that the solution of Baysilon OL-10% as a silicone leveling agent was removed in this experiment to avoid interference with the $-\text{Si-O-Si-}$ peak of the FTIR spectrum.

Creep-recovery test

A creep-recovery method (MARS-II, ThermoScientific, Germany) was employed using free-standing clearcoat films to investigate the creep compliance, $J(t)$, under a constant stress that stands for the degree of elasticity and the shear deformation.^{33,34} Thus, how the compliance data for cured clearcoats temporally changed with different polyisocyanates could be ascertained, reflecting the variation of crosslinked networks and viscoelastic properties of clearcoats. The films of approximately 300 μm thickness were produced by spraying clearcoats on the release paper and drying them at 140°C for over 20 min. Note that there was no

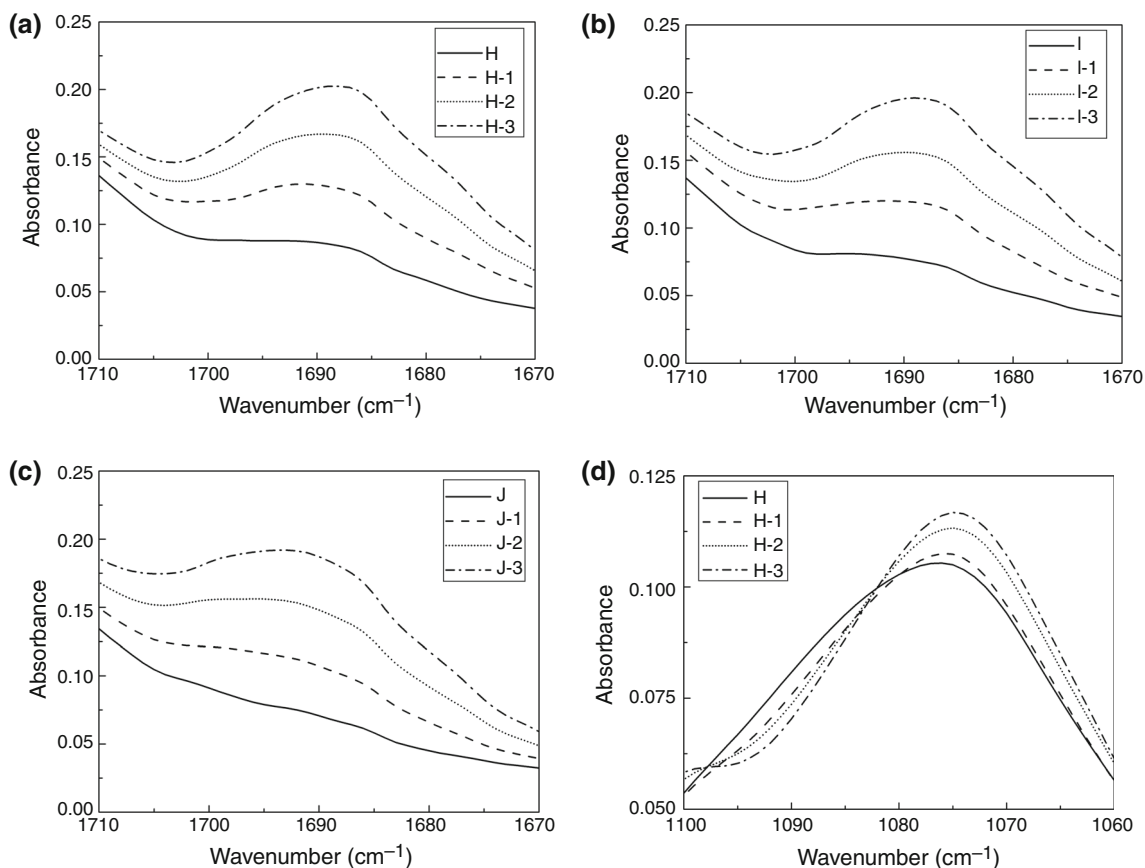


Fig. 2: FTIR spectra after thermal curing of clearcoats at 140°C: (a)–(c) –COO peaks (1690 cm⁻¹) in urethane bond [–NHCOO–] for H, I, and J-type clearcoats, and (d) –Si–O–Si– peaks (1080 cm⁻¹) for H-type clearcoats

residual solvent inside the dried clearcoat films under the given drying conditions.³⁵ Stresses (τ) were applied to 1×10^6 Pa and 2×10^6 Pa, and duration times for creep and recovery were 50 and 150 s, respectively. Note that all creep compliances were measured as a function of time at ambient temperature.

Scratch test

The scratch behaviors of clearcoats, including self-recovery or self-reflow phenomena, were examined using a nano-scratch tester (NST, Open Platform, CSM Instruments, Switzerland).^{1,6,8,11,14,26} A progressive deformation load was provided to initiate fractures and plastic deformations on the clearcoat surface. During the nano-scratch test, the normal force acting on the clearcoat surface was gradually raised from 1.0 to 20 mN, with a scanning load speed of 1 mN/min. A sphero-conical 90° nano-indenter probe with an indenter radius of 0.5 μ m was implemented for this test. The nano-indenter checked scratch depths [penetration depth (Pd) and recovery depth (Rd)] of each sample, according to the ASTM norm D7187. Depth profiles and three-dimensional images of scratch patterns of clearcoats with different blocked polyisocya-

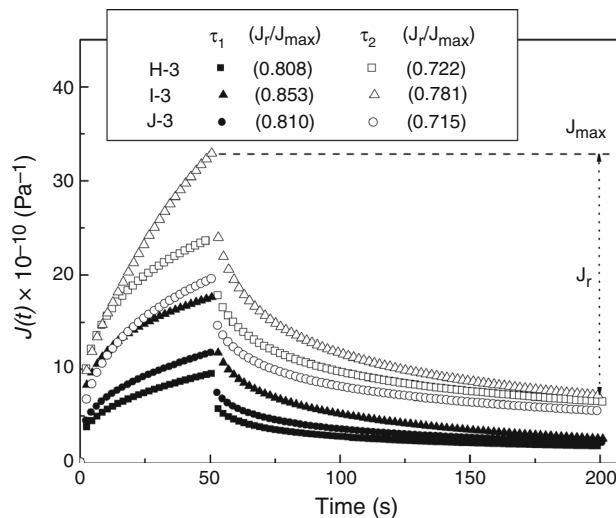


Fig. 3: Plots of $J(t)$ of clearcoat samples H-3, I-3, and J-3 from the creep test under constant stresses of 1.0×10^6 Pa (τ_1) and 2.0×10^6 Pa (τ_2)

nates under various scratch-healing temperature conditions were captured by contact mode AFM (Nanos, ScanPanel, Bruker, Germany), in connection

with a Peltier plate (PE94, Linkam, UK) to control the temperature range from 25 to 90°C.

Results and discussion

Curing analysis by RPT

Curing features of three clearcoat samples containing the highest portions of blocked polyisocyanate crosslinkers, named H-3, I-3, and J-3, were analyzed using the RPT to deduce changes in the extent of curing reactions, i.e., different formations of polymer crosslinked networks during the clearcoat curing, and flow resistance. Figure 1 shows a decrease of the oscillating period of the pendu-

lum for all samples, as the temperature was raised from 25 to 150°C. Furthermore, the decreasing pattern of the swinging period curves was shown to be quite dependent on the formulation of clearcoats with different kinds of blocked polyisocyanate crosslinkers. Sample H-3 was more reactive than samples I-3 and J-3 in that the curing curve for H-3 based on SMBI had a considerable descent owing to the increased networks. This is directly connected to the higher reactivity of the functional groups in SMBI, including two isocyanate functional groups and three additional alkoxyisilane functional groups.¹ SMBI can typically induce crosslinked networks through not only urethane bonds, but also inorganic bonds, via the attached alkoxyisilane functional groups, leading to improved mechanical properties, such as scratch resistance, as will be described later.

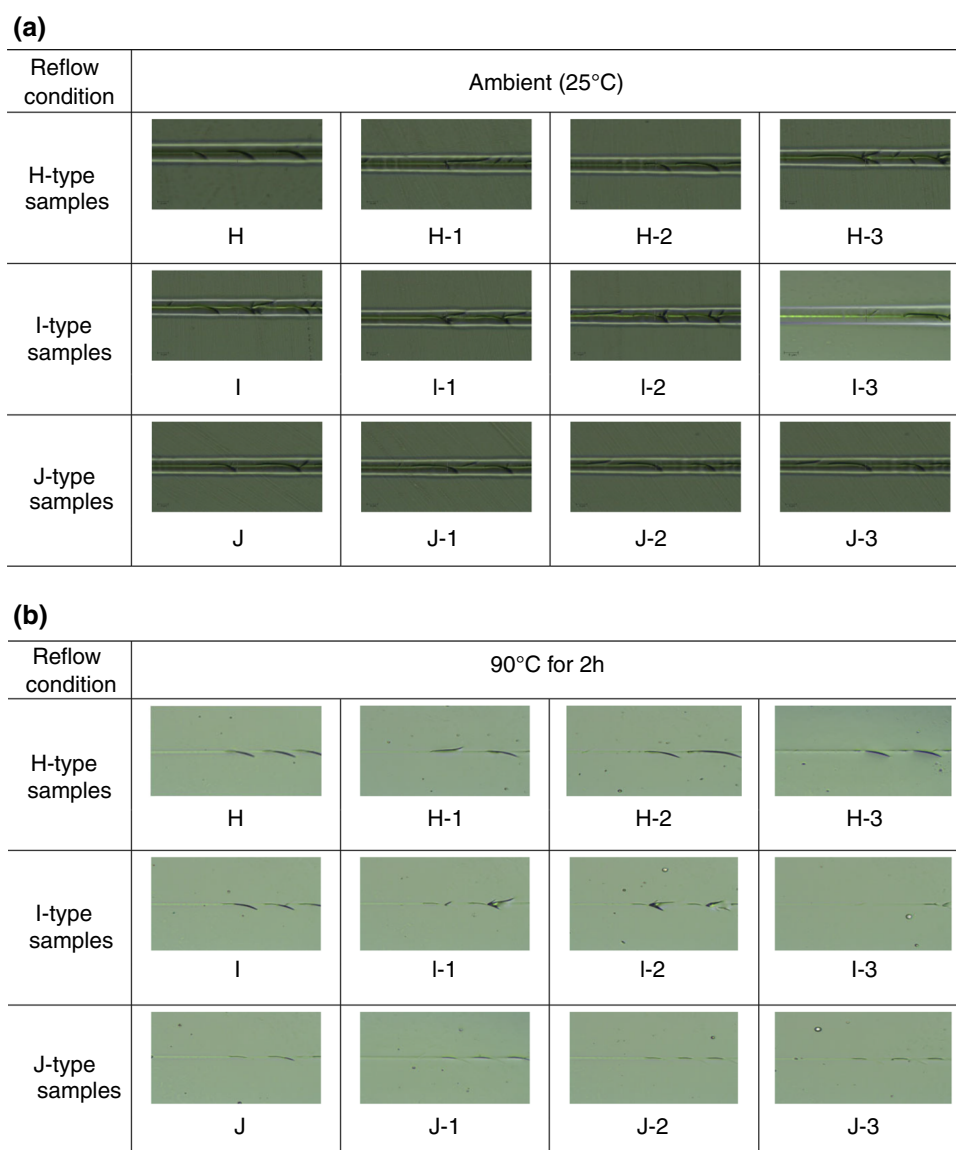


Fig. 4: Scratch patterns of H-, I-, and J-type clearcoat samples via nano-scratch test (200× magnifications using optical microscopy) under (a) ambient and (b) temperature conditions of 90°C for 2 h

FTIR analysis

Blocked polyisocyanates, including a number of isocyanate group blocking agents, can be dissociated when heated. After de-blocking at elevated temperatures, the released isocyanate groups react with the hydroxyl-terminated components of clearcoats to form a network of crosslinked urethane polymer structures. The de-blocking reaction can be easily identified by the appearance of the $-NCO$ group at 2270 cm^{-1} and the disappearance of the $-C=O$ group in the blocked $-NHCO$ group at 1720 cm^{-1} , as in the previous report.¹ Note that the de-blocking reaction was sub-

stantially activated over 120°C . Typically, crosslinking reactions forming urethane bonds gradually occur between the hydroxyl groups in acrylic polyol and the de-blocked $-COO$ ester groups in blocked polyisocyanate over 120°C . Figures 2a–2c show that absorption peaks at 1690 cm^{-1} for three sample groups, assigned to the carbonyl group of urethane ($-NH-COO-$) bonds, were considerably raised with the increasing amount of three blocked polyisocyanates. The absorption peaks at 1690 cm^{-1} for H-type clearcoats were slightly higher than the others, because these contained SMBI with both urethane and alkoxy-silane groups, exhibiting the silane-urethane hybrid

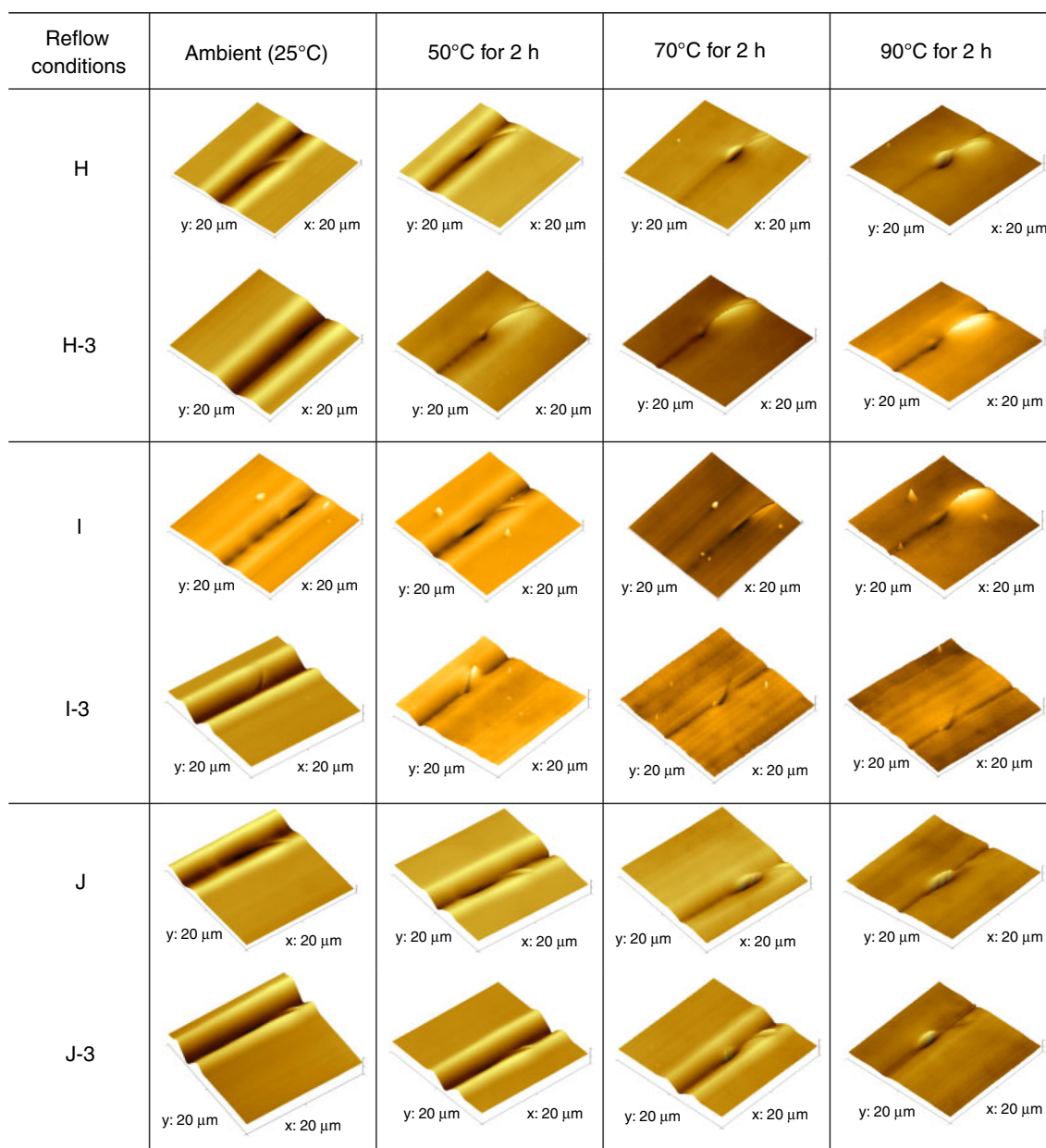


Fig. 5: Three-dimensional AFM scratch images of H-, I-, and J-type clearcoat samples at the lateral load of 10 mN in the nano-scratch test under ambient, 50, 70, and 90°C for 2 h, respectively

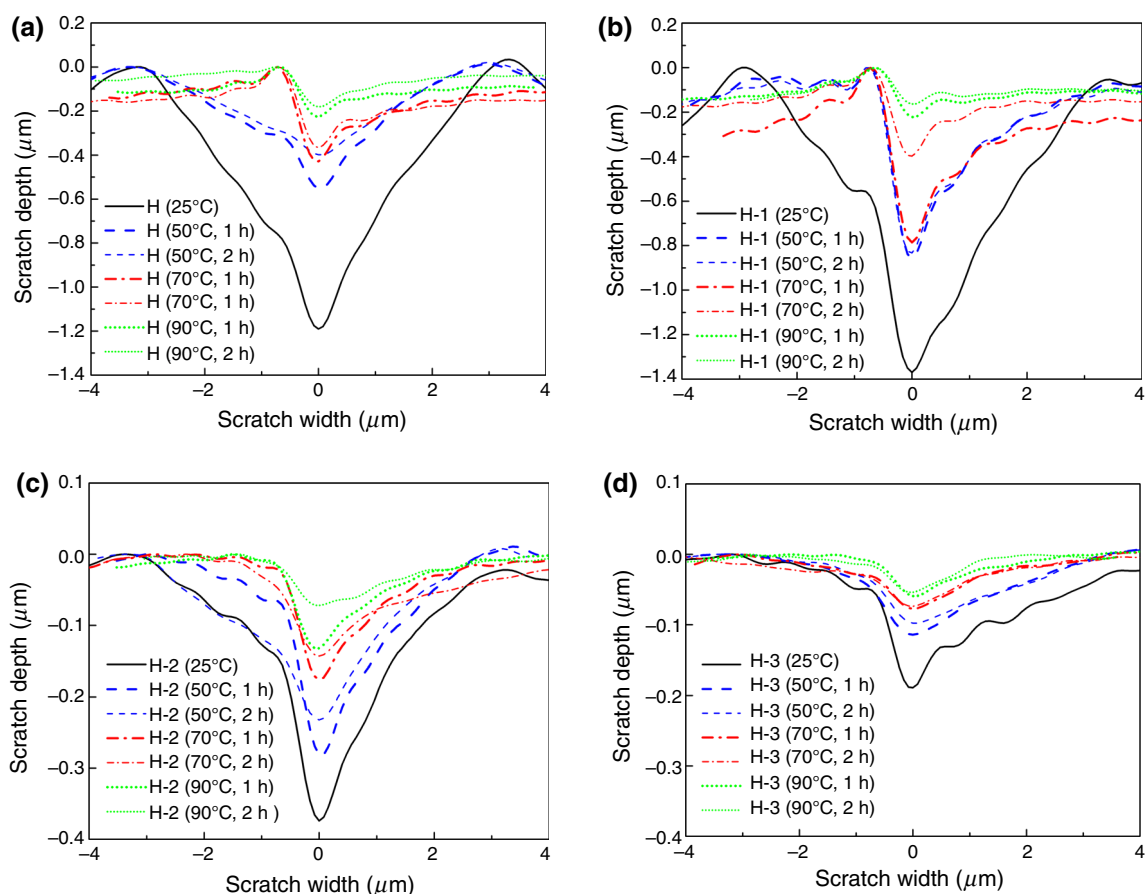


Fig. 6: Scratch-recovery profiles of H-type clearcoats with different contents of SMBI using the nano-scratch test and AFM at the lateral load of Lc1 under various temperatures and duration times

crosslinking. Three alkoxy silane groups of the SMBI additionally enhance the crosslinking density, either via hydrolysis and self-condensation reactions creating $-\text{Si}-\text{O}-\text{Si}-$ bonds, or reactions with the hydroxyl groups of the acrylic polyols. The generation of $-\text{Si}-\text{O}-\text{Si}-$ bonds in SMBI was corroborated by the FTIR spectra in Fig. 2d, in which the absorption peaks at 1080 cm^{-1} assigned to an $-\text{Si}-\text{O}-\text{Si}-$ vibration increased with the content of SMBI. These results identically correlated with the previous published data.¹

Creep-recovery properties

In order to qualitatively compare the change of elasticity and deformation of cured solid-like clearcoat films with different crosslinkers under room temperature conditions,^{33,34} creep-recovery measurements were performed under impartment (0–50 s) and release (50–200 s) of two constant stresses of $\tau_1 = 1 \times 10^6$ Pa and $\tau_2 = 2 \times 10^6$ Pa. Figure 3 displays the deformation and recovery features of H-3, I-3, and J-3 samples in terms of creep compliance, $J(t)$. Sample I-3, with considerable flexible chain structure, showed larger compliance when the stress was applied, and

larger recoverable behavior when the stress was released, than samples H-3 and J-3, considering the degree of recovery defined as J_r/J_{\max} . Here, J_{\max} and J_r denote the maximum $J(t)$ at 50 s and the difference between J_{\max} and $J(t)$ at 200 s, respectively. It should be mentioned here that the compliance curve for the H-3 sample was higher than that for the J-3 sample, when higher stress (τ_2) was applied, as opposed to the case under relatively lower stress condition (τ_1). This might be due to the relative response of rather flexible $-\text{Si}-\text{O}-\text{Si}-$ bonds in the H-3 sample.

Scratch resistance and recovery characteristics

The scratch behavior of clearcoats can be quantified in terms of the load at the first fracture (designated by Lc1), width and depth shapes of scratches, and scratch recovery. The transition from the plastic deformation to the fracture range is identified by the indentation depth profile under the given load, captured by the AFM. It is also crucial to consider the recovery characteristics of scratched clearcoats, as an indicator of their reflowability, when extrinsically triggered by the external heating process. Figure 4 illustrates the

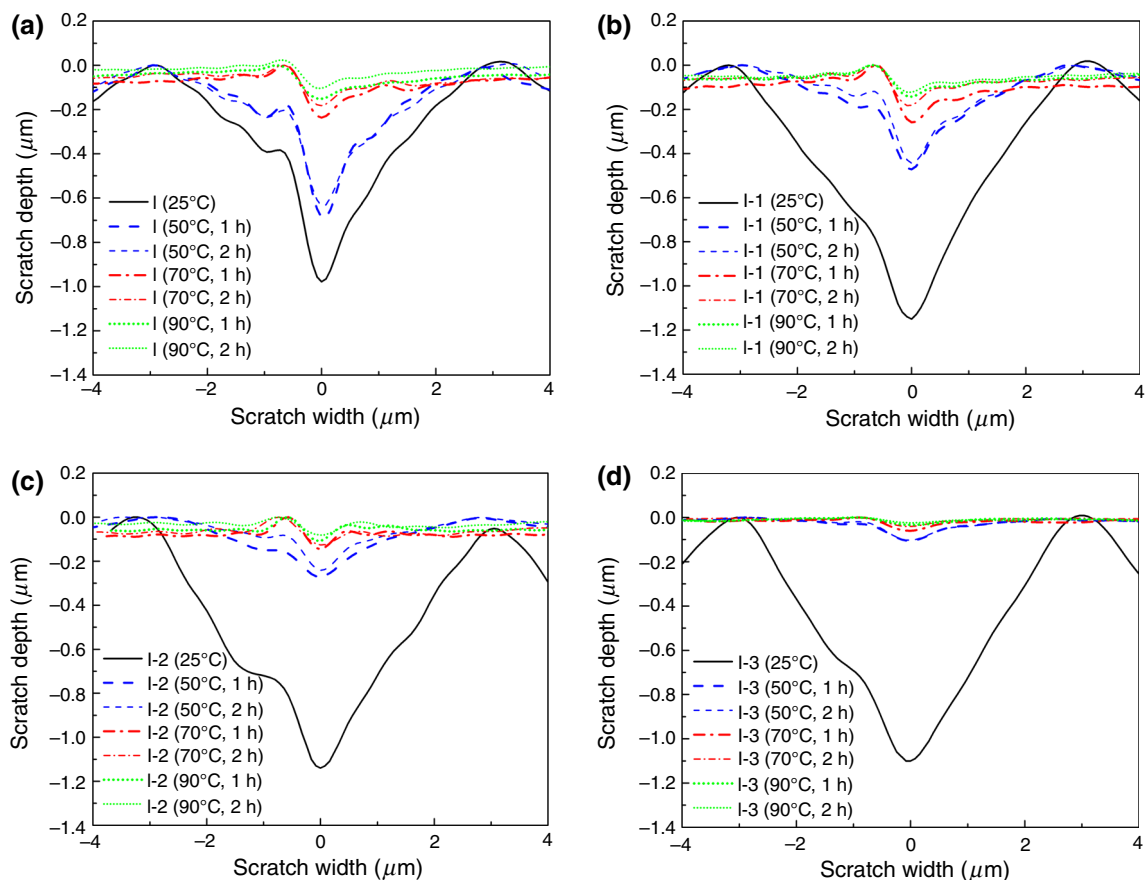


Fig. 7: Scratch-recovery profiles of I-type clearcoats with different contents of HDI using the nano-scratch test and AFM at the lateral load of Lc1 under various temperatures and duration times

comparison of fractured one-dimensional images at Lc1 of clearcoats with three different crosslinkers under the ambient conditions (Fig. 4a) and the reflow conditions at 90°C for 2 h (Fig. 4b), after the nano-scratch test within the range of lateral load from 1.0 to 20.0 mN. The recovery patterns of scratched clearcoats in Fig. 4b fairly reflect the intrinsic chemical structures of blocked polyisocyanate crosslinkers. I-type samples remarkably healed their scratched cracks, as the portion of HDI crosslinker increased, due to their typically plastic deformable characteristics endowed by linear aliphatic chains of HDI. Note that the effect of the portions of crosslinkers in H-type and J-type samples on the scratch recovery was not definitely discerned from these one-dimensional images, captured by conventional optical microscopy.

In order to analyze the effect of scratch recovery more systematically, the scratched substrates at 10 mN were annealed at ambient, 50, 70, and 90°C for 2 h, respectively. The subsequent full three-dimensional images via AFM depicted in Fig. 5 show that I and I-3 samples containing blocked HDI polyisocyanate were more notably recoverable from the main scratch lines, under various self-reflow temperature conditions. It is substantiated that the flexible linear aliphatic chemical chains with both hard and soft segments in the

polyurethane backbone (i.e., HDI) can effectively improve the capability to recover scratches induced by an external lateral force, in contrast with the aromatic chains of blocked polyisocyanates (i.e., SMBI and IPDI). In addition, the scratch-recovery effect was greatly enhanced over 70°C, regardless of the amount of blocked HDI polyisocyanate.

Samples H and H-3 with SMBI also exhibited moderate scratch-recovery ability in proportion to the given temperature conditions, which could be ascribed to polymeric networks formed by both the urethane and silanol bonds inside SMBI. The deep penetration and scratch fracture patterns for samples J and J-3 with IPDI still remained, even after annealing, in this case evidently indicating the fracture deformation mode rather than the plastic deformation mode.

The two-dimensional penetration depth profiles of scratches from the nano-scratch test were compared in detail using simultaneous visualized AFM under various conditions, i.e., self-reflow temperatures from ambient to 50, 70, and 90°C and duration times of 1 and 2 h, as portrayed in Figs. 6, 7, and 8. As the portion of SMBI in the clearcoat increased from H to H-3, penetration depths and widths of scratches at the lateral load of Lc1 were effectively alleviated, showing the increased external scratch resistance and scratch-

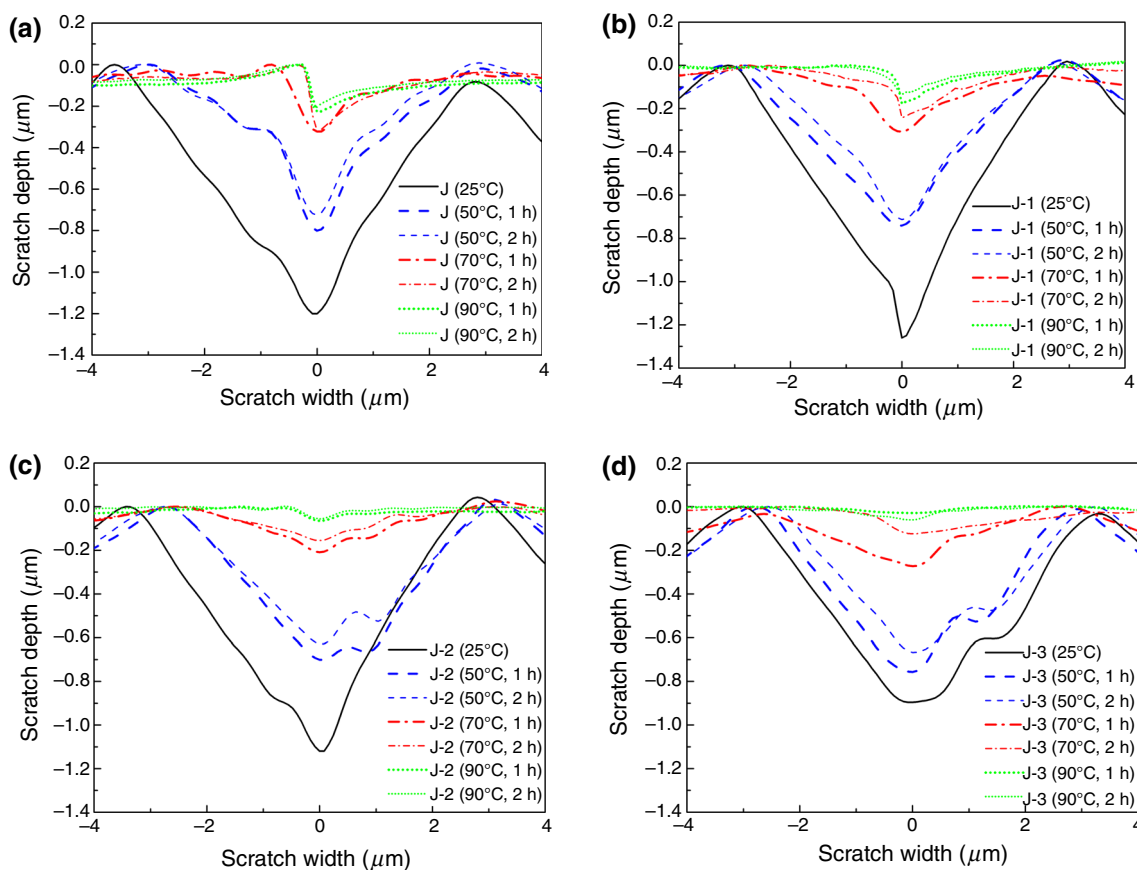


Fig. 8: Scratch-recovery profiles of J-type clearcoats with different contents of IPDI using the nano-scratch test and AFM at the lateral load of Lc1 under various temperatures and duration times

recovery features by the combination of urethane and silanol bonds; for instance, the penetration depth decreased from 1.2 to 1.4 μm for samples H and H-1, to 0.37 for H-2, and 0.19 μm for H-3, under ambient conditions. Reinforcement of SMBI in a clearcoat consistently improved penetration resistance and also gave an excellent scratch-recovery property along with the self-reflow temperatures and duration times (Fig. 6) due to the flexible $-\text{Si}-\text{O}-\text{Si}-$ bonds in H samples. These results were correlated with those from the creep-recovery test in Fig. 3. During the reflow stage, most of the scratch damages of sample H-2 could be healed up to satisfactorily reduced depths of 0.15 μm over 70°C for 1 h. Also, sample H-3, with the higher SMBI content, exhibited superb scratch resistance, resulting in smaller deformation and better recovery properties from its asymmetrical depth profiles.

As displayed in Fig. 7, penetration depths and widths of I-type clearcoat samples also showed better scratch-recovery effects in proportion to the amount of blocked HDI polyisocyanate under various temperatures and duration times. The influence of self-reflow conditions on the scratch recovery of I-type samples

was definitely superior to that of H- and J-type samples, due to their intrinsic linear aliphatic polymeric structure based on HDI. It is noteworthy to mention that I-type samples with a more flexible and ductile property did not show enhanced resistance to external scratch loads under the ambient conditions, despite the increase of the blocked HDI polyisocyanate.

J-type samples, based on blocked IPDI polyisocyanate, showed more significant cracking patterns, and less effective scratch-recovery features, even under the increased temperatures and duration times (Fig. 8). These characteristics were mainly ascribed to the polymeric structure of IPDI, derived from a cyclic structure, not playing an important role in the restoration of scratch damages. Furthermore, J-type samples gave relatively deep penetration and considerable residual depth patterns under various self-reflow temperatures and duration times, resulting from their fracture deformation feature. It is worth mentioning here that it will be helpful to further identify the temporal evolution of scratch and self-reflow properties of clearcoats during long-term aging in the next study.

Conclusion

The scratch characteristics of automotive clearcoats containing three different blocked polyisocyanate crosslinkers, namely SMBI, as well as conventional HDI and IPDI, accompanied with acrylic polyol and butylated melamine resins, were systematically investigated by means of a nano-scratch test in connection with AFM. The scratch performance and recovery features of various clearcoats were interpreted with changes in their own physical properties and reaction characteristics. It was revealed that SMBI crosslinker could considerably enhance the scratch resistance from nano-scratch tests in comparison with HDI and IPDI crosslinkers, as its portion increased; and also, it offered reasonable recoverable capability of a clearcoat by controlling external self-reflow temperature and duration time conditions. Due to the formation of urethane and silanol bonds by SMBI in the clearcoat, the scratch pattern relied more upon plastic deformation than fracture deformation in the range from low to high external shear force. The recovery nature of damaged scratches on the clearcoat surface might be closely related to the intrinsic polymeric structures of each crosslinker as well as the self-reflow conditions. Penetration depth profiles, and two- and three-dimensional images from nano-scratch tests combined with AFM, demonstrated indispensable data to figure out the role of three different crosslinkers on the scratch recovery of automotive clearcoats. The data acquired from the RPT test could competently reinforce the relationship between the formation of crosslinked polymeric networks inside clearcoats and their resulting scratch and recovery performance.

Acknowledgments This study was supported by research grants from the Industrial Strategic Technology Development Program (10035163), and the Human Resources Development Program of the Korea Institute of Energy Technology Evaluation and Planning (KETEP: No. 20134010200600).

References

1. Noh, SM, Lee, JW, Nam, JH, Park, JM, Jung, HW, "Analysis of Scratch Characteristics of Automotive Clearcoats Containing Silane Modified Blocked Isocyanates via Carwash and Nano-scratch Tests." *Prog. Org. Coat.*, **74** 192–203 (2012)
2. Wagner, G, Osterhold, M, "Comparison of Different Test Methods for Determining the Mar Resistance of Clearcoats." *Mat.-wiss. U. Werkstofftech.*, **30** 617–622 (1999)
3. Jardret, V, Lucas, BN, Oliver, W, "Scratch Durability of Automotive Clear Coatings: A Quantitative, Reliable and Robust Methodology." *J. Coatings Technol.*, **72** 79–88 (2000)
4. Kutschera, M, Sander, R, Herrmann, P, Wechenmann, U, Poppe, A, "Scratch Resistance of Automobile Clearcoats: Chemistry and Characterization on the Micro- and Nano-scale." *JCT Res.*, **3** 91–97 (2006)

5. Flosbach, C, Schubert, W, "Zero Etch Clear—A New Modular Clear Coat System with Excellent Scratch/mar Performance." *Prog. Org. Coat.*, **43** 123–130 (2001)
6. Jardret, V, Morel, P, "Viscoelastic Effects on the Scratch Resistance of Polymers: Relationship between Mechanical Properties and Scratch Properties at Various Temperatures." *Prog. Org. Coat.*, **48** 322–331 (2003)
7. Ramsteiner, F, Jaworek, T, Weber, M, Forster, S, "Scratch Resistance and Embrittlement of Coated Polymers." *Polym. Test.*, **22** 439–451 (2003)
8. Krupička, A, Johansson, M, Hult, A, "Use and Interpretation of Scratch Tests on Ductile Polymer Coatings." *Prog. Org. Coat.*, **46** 32–48 (2003)
9. Hainsworth, SV, Kilgallon, PJ, "Temperature-variant Scratch Deformation Response of Automotive Paint Systems." *Prog. Org. Coat.*, **62** 21–27 (2008)
10. Groenewolt, M, "Highly Scratch Resistant Coatings for Automotive Applications." *Prog. Org. Coat.*, **61** 106–109 (2008)
11. Seubert, CM, Nichols, ME, "Scaling Behavior in the Scratching of Automotive Clearcoats." *J. Coat. Technol. Res.*, **4** 21–30 (2007)
12. Hara, Y, Mori, T, Fujitani, T, "Relationship between Viscoelasticity and Scratch Morphology of Coating Films." *Prog. Org. Coat.*, **40** 39–47 (2000)
13. Osterhold, M, Wagner, G, "Methods for Characterizing the Mar Resistance." *Prog. Org. Coat.*, **45** 365–371 (2002)
14. Schulz, U, Wachtendorf, V, Klimmasch, T, Alers, P, "The Influence of Weathering on Scratches and on Scratch and Mar Resistance of Automotive Coatings." *Prog. Org. Coat.*, **42** 38–48 (2001)
15. Lange, J, Luisier, A, Hult, A, "Influence of Crosslink Density, Glass Transition Temperature and Addition of Pigment and Wax on the Scratch Resistance of an Epoxy Coating." *J. Coat. Technol.*, **69** 77–82 (1997)
16. Noh, SM, Lee, JW, Nam, JH, Byun, KH, Park, JM, Jung, HW, "Dual-curing Behavior and Scratch Characteristics of Hydroxyl Functionalized Urethane Methacrylate Oligomer for Automotive Clearcoats." *Prog. Org. Coat.*, **74** 257–269 (2012)
17. Evans, DC, Lancaster, JK, "The Wear of Polymers." *Treatise Mater. Sci. Technol.*, **13** 85–139 (1979)
18. Noh, SM, Min, J, Lee, JW, Jung, HW, Park, JM, "Application of Dual-function Microgels in Ultraviolet/thermal Dual-cure Clear Coats." *J. Appl. Polym. Sci.*, **126** E493–E500 (2012)
19. Park, S, Hwang, JW, Kim, KN, Lee, GS, Nam, JH, Noh, SM, Jung, HW, "Rheology and Curing Characteristics of Dual-Curable Clearcoats with Hydroxyl Functionalized Urethane Methacrylate Oligomer: Effect of Blocked Isocyanate Thermal Crosslinkers." *Korea-Aust. Rheol. J.*, **26** 159–167 (2014)
20. Amerio, E, Fabbri, P, Malucelli, G, Messori, M, Sangermano, M, Taurino, R, "Scratch Resistance of Nano-silica Reinforced Acrylic Coatings." *Prog. Org. Coat.*, **62** 129–133 (2008)
21. Anderson, LG, Barkac, KA, Chasser, AM, DeSaw, SA, Hartman, ME, Hayes, DE, Hockswender, TR, Kuster, KL, Montague, RA, Nakajima, M, Olson, KG, Richardson, JS, Sadvary, RJ, Simpson, DA, Tyebjee, S, Wilt, TF, "Cured Coatings Having Improved Scratch Resistance, Coated Substrates and Methods Thereto." US Patent #US6387519B1 (2002)
22. Seubert, C, Nichols, M, Henderson, K, Mechtel, M, Klimmasch, T, Pohl, T, "The Effect of Weathering and Thermal Treatment on the Scratch Recovery Characteristics of Clearcoats." *J. Coat. Technol. Res.*, **7** 159–166 (2010)
23. Yoon, JA, Kamada, J, Koynov, K, Mohin, J, Nicolay, R, Zhang, Y, Balaz, AC, Kowalewski, T, Matyjaszewski, K, "Self-healing Polymer Films Based on Thiol-Disulfide Exchange Reactions and Self-healing Kinetics Measured

- Using Atomic Force Microscopy.” *Macromolecules*, **45** 142–149 (2012)
24. Urban, MW, “Stratification, Stimuli-Responsiveness, Self-Healing, and Signaling in Polymer Networks.” *Prog. Polym. Sci.*, **34** 679–687 (2009)
25. Bauer, F, Glasel, H-J, Decker, U, Ernst, H, Freyer, A, Hartmann, E, Sauerland, V, Mehnert, R, “Trialkoxysilane Grafting onto Nanoparticles for the Preparation of Clear Coat Polyacrylate Systems with Excellent Scratch Performance.” *Prog. Org. Coat.*, **47** 147–153 (2003)
26. Krupička, A, Johansson, B, Johansson, M, Hult, A, “The Effect of Long-Term Recovery and Storage on the Mechanical Response of Ductile Poly(urethane) Coatings.” *Prog. Org. Coat.*, **48** 14–27 (2003)
27. Wicks, DA, Wicks, ZW, Jr, “Blocked Isocyanates III: Part A. Mechanisms and Chemistry.” *Prog. Org. Coat.*, **36** 148–172 (1999)
28. Wicks, DA, Wicks, ZW, Jr, “Blocked Isocyanates III: Part B: Uses and Applications of Blocked Isocyanates.” *Prog. Org. Coat.*, **41** 1–83 (2001)
29. Meier-Westhues, U, *Polyurethanes: Coatings, Adhesives, and Sealants*. Vincentz Network, Hannover, 2007
30. Bock, M, *Polyurethanes for Coatings*. Vincentz Network, Hannover, 2001
31. Kozakiewicz, J, Przybylski, J, Sylwestrzak, K, Ofat, I, “New Family of Functionalized Crosslinkers for Heat-curable Polyurethane Systems—A Preliminary Study.” *Prog. Org. Coat.*, **72** 120–130 (2011)
32. Moon, J-I, Lee, Y-H, Kim, H-J, Noh, SM, Nam, JH, “Synthesis of Elastomeric Polyester and Physical Properties of Polyester Coating for Automotive Pre-primed System.” *Prog. Org. Coat.*, **75** 65–71 (2012)
33. Ueda, K, Kanai, H, Amari, T, “Viscoelastic Properties of Paint Films and Formability in Deep Drawing of Pre-painted Steel Sheets.” *Prog. Org. Coat.*, **45** 15–21 (2002)
34. Mott, PH, Rizos, A, Roland, CM, “Optical Birefringence of Polyisobutylene During Creep and Recovery.” *Macromolecules*, **34** 4476–4479 (2001)
35. Hwang, H-D, Park, C-H, Moon, J-I, Kim, H-J, Masubuchi, T, “UV-Curing Behavior and Physical Properties of Waterborne UV-Curable Polycarbonate-Based Polyurethane Dispersion.” *Prog. Org. Coat.*, **72** 663–675 (2011)